JACS
JOURNAL OF THE AMERICAN CHEMICAL SOCIETY
Article
pubs.acs.org/JACS

Electrochemical Measurements of the Kinetics of Inhibition of Two FeFe Hydrogenases by O_2 Demonstrate That the Reaction Is Partly Reversible

Christophe Orain,[†] Laure Saujet,[‡,§] Charles Gauquelin,[∥] Philippe Soucaille,[∥] Isabelle Meynial-Salles,[∥] Carole Baffert,[†] Vincent Fourmond,[†] Hervé Bottin,[‡,§] and Christophe Léger*[,†]

[†]Laboratoire de Bioénergétique et Ingénierie des Protéines, CNRS/Aix-Marseille Université, 13402 Marseille, France
[‡]CEA, Institut de Biologie et de Technologies de Saclay IBITECS, SB2SM, F-91191 Gif sur Yvette, France
[§]Institut de Biologie Intégrative de la Cellule I2BC, UMR 9198, CEA, CNRS, Université Paris Sud, F-91191 Gif sur Yvette, France
[∥]Université de Toulouse, INSA, UPS, INP, LISBP, INRA:UMR792,135 CNRS:UMR 5504, avenue de Rangueil, 31077 Toulouse, France

ABSTRACT: The mechanism of reaction of FeFe hydrogenases with oxygen has been debated. It is complex, apparently very dependent on the details of the protein structure, and difficult to study using conventional kinetic techniques. Here we build on our recent work on the anaerobic inactivation of the enzyme [Fourmond et al. *Nat. Chem.* **2014**, *4*, 336−342] to propose and apply a new method for studying this reaction. Using electrochemical measurements of the turnover rate of hydrogenase, we could resolve the first steps of the inhibition reaction and accurately determine their rates. We show that the two most studied FeFe hydrogenases, from *Chlamydomonas reinhardtii* and *Clostridium acetobutylicum*, react with O_2 according to the same mechanism, despite the fact that the former is much more O_2 sensitive than the latter. Unlike often assumed, both enzymes are *reversibly* inhibited by a short exposure to O_2. This will have to be considered to elucidate the mechanism of inhibition, before any prediction can be made regarding which mutations will improve oxygen resistance. We hope that the approach described herein will prove useful in this respect.

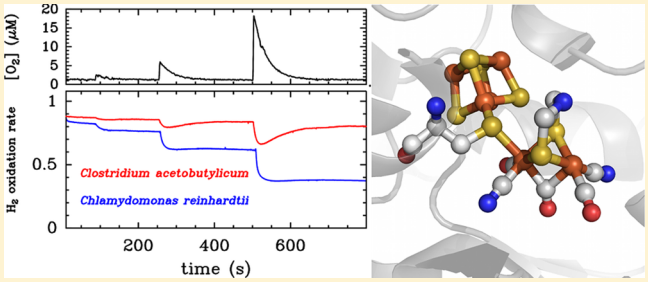

1. INTRODUCTION

Hydrogenases,[1] the enzymes that oxidize or produce H_2, are classified into two main classes, depending on metal content.[2] This paper deals with FeFe hydrogenases, whose active site, the so-called "H cluster", consists of a $[Fe_2(CO)_3(CN)_2(dtma)]$ subsite (dtma = dithiomethylamine)[3−5] covalently bound to a [4Fe4S] subcluster (Figure 1). Other hydrogenases use a binuclear cluster of Ni and Fe. In addition to studies of their catalytic mechanism, the characterization of the inactivation of hydrogenases by O_2 has become a major field of academic research. The reason for this is that inactivation by O_2 is considered a major obstacle if one ever wants to use hydrogenases for biological or biotechnological H_2 oxidation or (photo)production.[6−8]

That FeFe hydrogenases are O_2 sensitive is clear from the observation that, unlike NiFe hydrogenases, they have to be purified under fully anaerobic conditions.[9] This is not because they are inhibited more quickly than other hydrogenases,[11] but because FeFe hydrogenases react with O_2 to produce some inactive forms of the enzyme that cannot be reactivated. The nature of these end-products and the mechanism of the reaction are still debated. From the results of electrochemical measurements, we showed that the aerobic inactivation of the enzyme from *Clostridium acetobutylicum* (Ca) occurs as a result of initial, slow, and reversible formation of an O_2 adduct, followed by an irreversible transformation.[12] That O_2 initially targets the distal Fe of the 2Fe subsite is clear from the observation that the competitive inhibitor CO binds on this atom in the crystal[13] and protects the enzyme from O_2 inactivation.[12,14] This is also supported by several theoretical investigations.[15−19] The fact that all studies agree about the initial site of O_2 attack is relevant to the engineering of FeFe-hydrognases that will be more resistant to O_2. In particular, based on the observation that electron transfer from the di-iron subsite to O_2 makes oxygen attachment thermodynamically favorable, Blumberger and co-workers proposed that mutations that counteract this electron transfer may increase oxygen resistance.[19] This working hypothesis should now be tested by characterizing the kinetics of inhibition of site-directed mutants.

The fate of the O_2 adduct that is formed in the first step of the reaction with O_2 is still debated. Haumann and co-workers have used X-ray absorption spectroscopy to characterize the enzyme from *Chlamydomonas reinhardtii* exposed to O_2, and

Received: July 3, 2015
Published: September 9, 2015

DOI: 10.1021/jacs.5b06934
J. Am. Chem. Soc. 2015, 137, 12580−12587

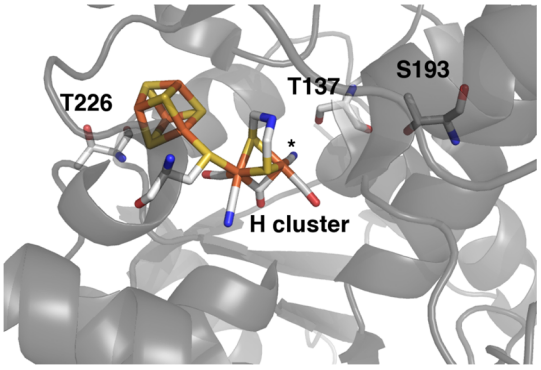

Figure 1. Model of the structure of the H-cluster of *Chlamydomonas reinhardtii* (Cr) FeFe hydrogenase and the surrounding proteic matrix. An asterisk marks the binding site for substrate H_2 or inhibitors O_2 or CO.[12,13] We also show the nonconserved threonine that is recognized in ref 19 and replaced with a lysine in this work (T226K mutant), and the conserved threonine and serine residues (residues 137 and 193) mentioned in ref 20. The image was made using pdbs 3LX4[21] and 3C8Y,[22] replacing the bridging oxygen atom with a nitrogen.[5,23] The figure was made with PyMol.

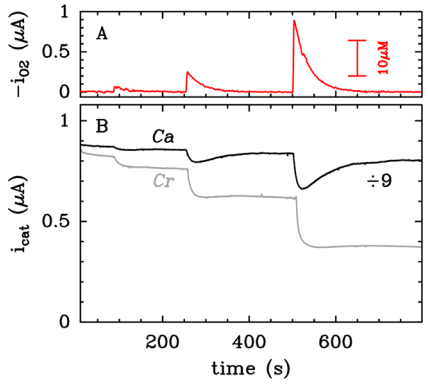

Figure 2. Ca and Cr FeFe hydrogenases behavior upon exposure to O_2, T = 12 °C, 1 bar H_2, pH = 7. (A) O_2-reduction current on a rotating graphite electrode against time, E = −560 mV, ω = 6000 rpm. (B) Catalytic H_2 oxidation current against time for Ca (black) and Cr (gray) FeFe hydrogenases, E = 40 mV, electrode rotation rate ω = 3000 rpm, $[O_2]_0$ = 1.25, 6.25, and 22 μM. Values of τ measured from the O_2 reduction signal were 18, 33, and 33 s for the experiment with Ca hydrogenase, and 30, 24, and 25 s for the experiment with Cr hydrogenase.

they concluded that the reactive oxygen species formed upon reaction of O_2 at the distal Fe react on the 4Fe4S subcluster, which is irreversibly damaged.[14,24] The recent crystal structure of the same enzyme treated with O_2 suggests otherwise: it shows an intact 4Fe4S subcluster, no 2Fe subcluster, and an oxidized cysteine.[25]

Using kinetic methods for learning about a mechanism generally requires that one analyzes the progress of a reaction with a model to measure rate constants, and examines how these rate constants depend on the experimental parameters. This justifies the need for analytical methods that make it possible to precisely characterize the kinetics of reaction of hydrogenases with O_2. However, this reaction is difficult to study using traditional methods for several reasons. Most obviously, dioxygen oxidizes quickly the soluble redox partners of hydrogenase, and therefore, solution assays that rely on monitoring the redox partner concentration can only be performed under fully anaerobic conditions. Second, the activity must be sampled at a relatively high frequency in order to measure the rate of inactivation; however, the reaction with O_2 is fast on the time scale of solution assays.

Direct electrochemistry has been very useful for studying the kinetics of reaction of hydrogenases with O_2 because when the enzyme directly transfers electrons to an electrode, the activity is simply measured as a current which can be sampled at a high rate; moreover, the electrode potential can be set to a value at which O_2 reduction is slow and does not interfere with the measurement. We have shown that experiments where the enzyme is exposed to a controlled "burst" of O_2 concentration are easily designed and interpreted:[11,12,26] in a typical experiment, the enzyme is adsorbed or attached to a rotating electrode, in a solution that is being purged with H_2; a gastight syringe is used to inject a small amount of solution saturated with for example, air or O_2, while the electrode is spun at a high rate to minimize mass transport control of substrate and homogenize the inhibitor concentration; the concentration of O_2 increases in about 0.1 s and then decreases exponentially (see the discussion of Figure 2 in ref 26 and Figure 2A herein) as the solution re-equilibrates with the H_2 atmosphere. The activity of the enzyme is simultaneously monitored as a H_2 oxidation current, the change of which reports on the rate of inhibition.

In the particular case of FeFe hydrogenase, a complication is that the enzyme also inactivates under oxidizing *anaerobic* conditions in a complex process, which results in a multiphasic, background current decay[29] that is altered by the exposure to O_2. In voltammetric experiments, where the electrode potential is swept up and down, this oxidative inactivation appears as a strong hysteresis in the high-potential region; the departure from steady-state is all the more pronounced that the scan rate is slow, and of course this informs on the kinetics of (in)activation (e.g., Figure 4A).[27,28] The reversible, oxidative formation of inactive states is also detected in chronoamperometry experiments (CA), where the current decreases (respectively, increases) when the potential is stepped up (respectively, down), as observed in Figure 4B. In the case of *Chlamydomonas reinhardtii* (Cr) FeFe hydrogenase, the anaerobic inactivation is particularly fast,[29] which makes any quantification of the kinetics of aerobic inactivation tricky.

By combining accurate and quantitative electrochemical measurements, site-directed mutagenesis experiments and MD and DFT theoretical calculations, we have recently elucidated the molecular mechanism of oxidative anaerobic inactivation of FeFe hydrogenases.[29,30] This reaction is a multistep process which forms two inactive states that are protected against O_2 damage and can be reactivated when the potential is made more negative; a third inactive state is irreversibly formed under oxidizing conditions even in the absence of O_2 and H_2[29] (this anaerobic damage is seen in electrochemistry experiments[29] and also in titrations followed by FTIR,[23] unless the bridging amine group is changed from NH to CH_2, c.f. Figure 7A in ref 31.) It is now possible to combine anaerobic and aerobic inactivation in a single model that can be used to interpret the activity decay when the enzyme is exposed to O_2 at high electrode potential.

Here we show how to proceed, and we use this new strategy to compare the kinetics and mechanism of inhibition by O_2 of *Clostridium acetobutylicum* (Ca) and *Chlamydomonas reinhardtii* (Cr) FeFe hydrogenases. We also characterize a mutant of Cr FeFe hydrogenase, T226K (Thr226 is equivalent to Thr356 in

DOI: 10.1021/jacs.5b06934
J. Am. Chem. Soc. 2015, 137, 12580−12587

Clostridium pasteurianum (Cp) FeFe hydrogenase), where a positive charge is introduced near the cubane of the H-cluster in an (unsuccessful) attempt to slow down O_2 binding.

2. RESULTS

Figure 2 shows the results of two experiments aimed at comparing the O_2 sensitivity of Cr and Ca FeFe hydrogenases. In both cases, the electrochemical cell was housed in an anaerobic glovebox, and the enzyme was covalently attached to a rotating graphite disk electrode (WE1 in Figure 3),[32] which

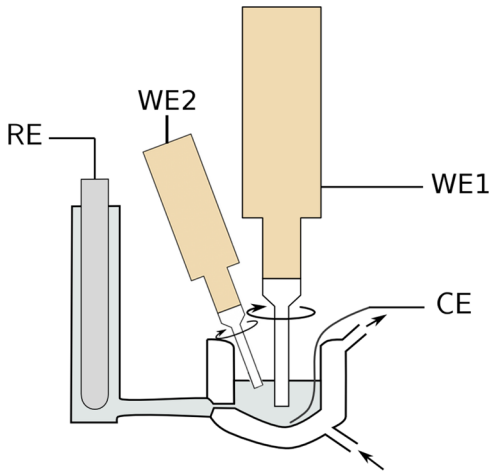

Figure 3. Two-compartment, two-RDE cell that we used for simultaneously monitoring the turnover rate and the concentration of O_2. The rotation of both working electrodes (WE) ensures that the concentrations of H_2 and O_2 are homogeneous in the bulk of the electrochemical cell (far from the electrode surfaces). Near the surface of the enzyme electrode (WE1), the concentrations remain close to those in the bulk (there is little H_2 depletion and no O_2 depletion). Near the O_2-reducing electrode (WE2), which is polarized at very low potential, the O_2 concentration drops to zero, but the O_2 reduction current is proportional to the bulk concentration of O_2 (ref 33).

was spun at a high rate in a buffer saturated with H_2. Panel B shows the catalytic H_2-oxidation response (turnover rate) against time, when the enzyme is inhibited by repeatedly injecting small amounts of O_2 saturated solution in the electrochemical cell. The electrode that supports the enzyme is poised at high electrode potential (40 mV, pH 7, T = 12 °C) to provide the driving force for H_2 oxidation and to prevent direct O_2 reduction on the enzyme electrode (else, this would add a negative contribution to the measured current, decrease the concentration of O_2 that the enzyme experiences, and produce reactive oxygen species that may also damage the enzyme). The negative slope to the H_2 oxidation current vs time trace before O_2 addition (also apparent in Figures 4D and 6D) results from the oxidative, anaerobic, reversible and irreversible inactivation of the enzyme, which is also clear in chronoamperometry experiments where no O_2 is added (e.g., Figures 4B and 5B). This background decay in current before O_2 is added is fully taken into account in the method we propose below.

With the setup we used here, and in contrast to our previous investigations, a second rotating disk working electrode (WE2 in Figure 3), made of just bare pyrolytic edge graphite and poised at low potential (−560 mV vs SHE), was spun in the same electrochemical cell to record an O_2-reduction current. According to the Levich equation, at a given electrode potential

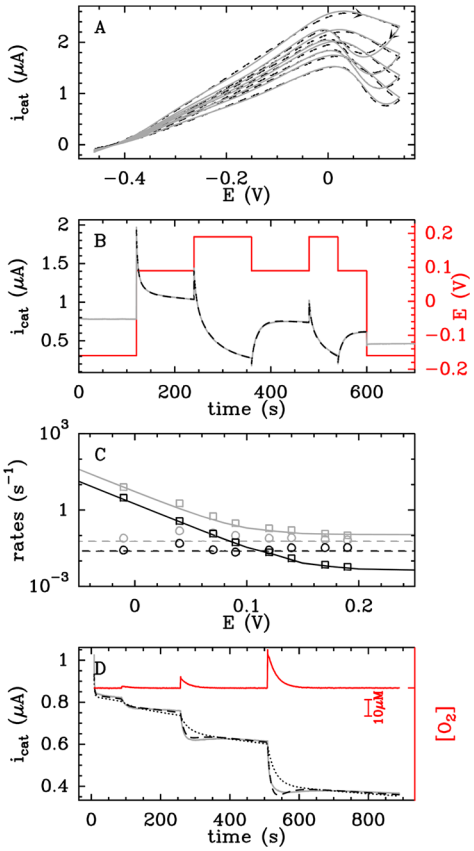

Figure 4. Characterization of the anaerobic/aerobic inhibition of Cr FeFe hydrogenase grafted on rotating disk electrode, T = 12 °C, pH = 7, ω = 3000 rpm, 1 bar H_2. (A) Cyclic voltammograms at different scan rates (20, 10, 5, and 2 mV/s; gray lines) and fits (dashed black lines; for kinetic model, see ref 29). (B) Current response of H_2-oxidation (gray line) and fit (black dashed line) for a sequence of potential steps applied to the electrode (red line). (C) Potential dependence of the rate constants for the anaerobic inactivation, extracted from fits shown on panel A ($k_a'(E)$ and $k_a''(E)$, plain lines and $k_i'(E)$ and $k_i''(E)$, dashed lines) and panel B ($k_a'(E)$ and $k_a''(E)$, square dots and $k_i'(E)$ and $k_i''(E)$, circle dots). The rate constants for the two species involved in the kinetic model are distinguished using black and gray plots. (D) Catalytic current of H_2-oxidation changes with enzyme exposure to O_2 (gray line, same data as in Figure 2B), E = 40 mV; $[O_2]_0$ = 1.25 μM, τ = 30 s; 6.25 μM, 25 s; 22 μM, 25 s. The dashed line is the best fit obtained using the kinetic model described in eq 2. Dotted line is the fit obtained with the same model setting k_a to 0. The oxygen reduction current is plotted against time as a red line, E = −560 mV; ω = 6000 rpm.

and electrode rotation rate, the value of this current is proportional to the instant concentration of O_2.[33] This signal in Figure 2A shows that the O_2 concentration increases quickly after each injection (the mixing time is lower than 0.1 s), and then decreases exponentially over time, as O_2 is flushed away by the stream of H_2,[26] according to

$$[O_2](t) = [O_2]_0 \exp[-(t - t_0)/\tau] \quad (1)$$

where $[O_2]_0$ is the concentration of O_2 at t_0, the time of injection, and τ is the time constant of the decay. The rotation of the electrode ensures instant homogenization. The value of τ can be measured by simply fitting an exponential to each relaxation of the O_2-reduction current. In the method we used previously,[11,12,26] we did not measure the concentration of O_2;

DOI: 10.1021/jacs.5b06934
J. Am. Chem. Soc. 2015, 137, 12580−12587

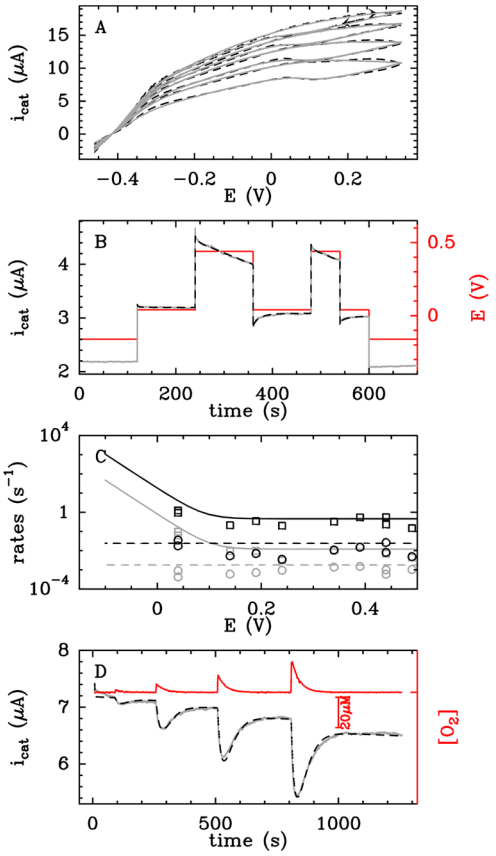

Figure 5. Characterization of the anaerobic/aerobic inactivation of Ca FeFe hydrogenase grafted on rotating electrode, T = 12 °C, pH = 7, ω = 3000 rpm, 1 bar H_2. (A) Cyclic voltammograms at different scan rates (10, 5, 2, and 1 mV/s; gray lines) and fits (dashed black lines). (B) Current response of H_2-oxidation (gray line) and fit (black dashed line) for a sequence of potential steps applied to the electrode (red line). (C) Potential dependence of the rate constants for the anaerobic inactivation, extracted from fits shown on panel A ($k_a'(E)$ and $k_a''(E)$, plain lines and $k_i'(E)$ and $k_i''(E)$, dashed lines) and panel B ($k_a'(E)$ and $k_a''(E)$, square dots and $k_i'(E)$ and $k_i''(E)$, circle dots). Rate constants for two species involved in the kinetic model are distinguished using black and gray plots. (D) Catalytic current of H_2-oxidation changes with enzyme exposure to O_2 (gray line, the data set is distinct from that in Figure 2B), E = 40 mV; $[O_2]_0$ = 1.25 μM, τ = 25 s; 6.25 μM, 32 s; 12.5 μM, 31 s; and 20 μM, 32 s. The O_2 reduction current is plotted against time as a red line, E = −560 mV; ω = 6000 rpm.

we just knew that it changed according to eq 1, and the value of τ had to be adjusted in the fitting procedure.

The magnitude of the reduction current is small enough that O_2 reduction does not significantly contribute to decreasing the concentration of O_2. For example, the third peak in Figure 2A follows an injection of 200 nmol of O_2 in the electrochemical cell. The charge under this peak is 30 μC, corresponding to the four-electron reduction of about 0.1 nmol of O_2. Therefore, the concentration of O_2 decreases because the cell solution equilibrates with the anaerobic atmosphere above the solution, *not* because O_2 is reduced on the second rotating disc electrode.

Figure 2B shows that the two enzymes behave very differently upon exposure to O_2: all things being equal,[34] the H_2-oxidation current decreases more in the case of Cr hydrogenase than with Ca hydrogenase, showing that the former enzyme is somehow more strongly inhibited than the latter. Moreover, Cr hydrogenase appears to react irreversibly with O_2 (however, see below), whereas a large fraction of the activity of Ca hydrogenase is recovered each time O_2 is removed from the solution. We shall clarify below the origin of this difference between the two enzymes.

Since we now fully understand the kinetics of anaerobic inactivation of FeFe hydrogenase,[29] it should be possible to fit to the current traces in Figure 2B a full kinetic model that accounts for anaerobic and aerobic inhibition. The two processes must be simultaneously taken into account because they are not independent; indeed, the inactive states that are reversibly formed upon anaerobic oxidation are protected against O_2.[29] The difficulty is to make sure that the fitting procedure can determine the many parameters that have to be simultaneously adjusted. We could solve this indetermination problem by independently measuring some of the kinetic parameters, the values of which we kept fixed in the fitting procedure aimed at quantifying the effect of O_2. The four panels of Figures 4 and 5 illustrate the procedure which we used to characterize each enzyme. (The data in Figure 4 were obtained with Cr FeFe hydrogenase; Figure 5 shows the results of a similar series of experiments, but carried out with the enzyme from Ca.)

(1) We recorded cyclic voltammograms (CVs) at various scan rates, and fitted the model in ref 29 to the complete set of CVs (panel A) to determine the parameters that define the dependence on potential of the kinetics of anaerobic inactivation:[29] the two first order rate constants of reversible anaerobic inactivation (k_i' and k_i''); the four parameters that define the two first order rate constants of reactivation after anaerobic inactivation $k_a'(E)$ and $k_a''(E)$ (the plateau values that are reached at high E and the values of the rates at 0 V vs SHE); the rate constant of irreversible inactivation at 0 V, $k_{irrev}^{@0V}$ (the rate at any other potential is obtained using $k_{irrev}(E) = k_{irrev}^{@0V} \times \exp(FE/2RT)$). See Methods. (2) To confirm the value of these parameters and make sure they are unique, we independently determined them a second time by analyzing chronoamperometry anaerobic experiments such as those in panel B. The details of the fitting procedures are in the Supporting Information of ref 29. Figure 7 also depicts all the oxidative transformations of the H cluster and defines the rate constants which we use in this text. Panel C compares the dependence on E of the anaerobic kinetic parameters (k_i', k_i'', k_a', k_a'') measured using either method. In the case of Ca FeFe hydrogenase, the *reversible* anaerobic inactivation is difficult to study because the *irreversible* anaerobic inactivation reaction dominates. We found that CA experiments cannot be used to measure the anaerobic rates of reversible (in)activation at low potential (below 0 V vs SHE) because the magnitude of the reversible change in current is small and difficult to distinguish from the background capacitive current when the potential is low and the reactivation fast; so the CA experiment in Figure 5B,C can only be used to confirm that the rates measured by fitting the CVs are correct, not to measure them independently. (3) We ran aerobic experiments such as those in Figure 2, and used the current signal recorded on the second working electrode to measure the values of τ in eq 1 (red line in Figures 4D and 5D). (4) We fitted the model below to these data,

$$\text{inactive} \overset{\text{anaerobic}}{\rightleftharpoons} \text{active} \underset{k_a}{\overset{k_i \times [O_2]_0 \exp^{-\frac{t-t_0}{\tau}}}{\rightleftharpoons}} O_2 \text{ adduct} \xrightarrow{k_3} \text{dead-end} \quad (2)$$

adjusting a single set of only four parameters (all others having been independently determined): the second order rate constant of reaction with O_2, k_i; the first-order rate of O_2

DOI: 10.1021/jacs.5b06934
J. Am. Chem. Soc. 2015, 137, 12580−12587

Table 1. Rates of Reaction with O_2 of the FeFe Hydrogenases from Ca, Cr, and Dd[a]

enzyme	k_i (s^{-1} mM^{-1})	k_a (s^{-1})	k_3 (s^{-1})	$k_i k_3/(k_3 + k_a)$ (s^{-1} mM^{-1})	conditions	ref
Ca	1.1 ± 0.2	0.04 ± 0.02	0.003 ± 0.002	0.077	+40 mV, pH 7, 12 °C	this work
Cr	2.5 ± 0.5	0.035 ± 0.005	0.024 ± 0.003	1.02	+40 mV, pH 7, 12 °C	this work
Cr T226K	2.8 ± 0.2	0.025 ± 0.005	0.015 ± 0.001	1.05	+40 mV, pH 7, 12 °C	this work
Ca	3.2	0.3	0.004	0.04	+200 mV, pH 7, 30 °C	12[b]
Ca	2.5 ± 0.4	0.30 ± 0.05			+200 mV, pH 7, 30 °C	11[b]
Dd	40 ± 8	0.15 ± 0.05			+200 mV, pH 7, 30 °C	11[b]
Ca				0.005 ± 0.001	+50 mV, pH 6, 10 °C	36[c]
Cr				0.2 ± 0.1	+50 mV, pH 6, 10 °C	36[c]
Dd				1.8 ± 0.3	+50 mV, pH 6, 10 °C	36[c]
Ca				0.006	pH 8, 4 °C	25[c]
Cr				0.2	pH 8, 4 °C	25[c]

[a]Values are taken from the literature or determined in this work, as indicated. [b]In our previous work (refs 11 and 12), the anaerobic inactivation was taken into account in a phenomenological manner,[37] the enzyme from Cr could not be studied because this inactivation is very fast, and the time-dependent O_2 concentration was not independently measured. [c]In the experiments carried out by others, the O_2 concentration is constant and only an apparent bimolecular rate of inhibition could be measured.[25,36]

dissociation, k_a, which accounts for the reactivation of the enzyme after O_2 is removed from the solution; the first-order rate of irreversible inactivation, k_3, that accounts for the fact that some of the activity is irreversibly lost after O_2 is flushed away from the solution; one parameter (k_{irrev}) that describes the irreversible anaerobic inactivation and should be determined from the analysis of the anaerobic experiments, but we found that we needed such small degree of liberty to fit the model to the data recorded under aerobic conditions.

The analysis of data such as those in Figures 4D and 5D returned the values of k_i, k_a, and k_3, at pH 7, T = 12 °C, E = 40 mV, reported in Table 1, rows 1 and 2.

Since the data in Figure 2B and Table 1 show that Cr FeFe hydrogenase reacts with O_2 much less reversibly than the enzyme from Ca, we wondered whether the inhibition of Cr hydrogenase could be simply treated as an irreversible bimolecular reaction with O_2. However, a close examination of the raw signals obtained with Cr hydrogenase in Figures 2B and 4D reveals a faint increase in current each time oxygen is flushed away; moreover, the dotted line in Figure 4D shows the poor result of a fit where we forced k_a = 0, showing that the reversibility of the inhibition has to be taken into account, even in the case of the enzyme from Cr.

In a previous theoretical investigation of O_2 binding to the H-cluster of hydrogenase, Blumberger and co-workers have suggested that using site-directed mutagenesis to introduce a positively charged amino acids near the cubane should make O_2 binding less favorable. They suggested replacing the non-conserved Thr356 (Figure 1) or Ser357 residues with a Lysine (Cp numbering; Thr226 and Arg227 in the enzyme from Cr, Ile235 and Ala236 in Dd). We constructed and purified the T226K mutant of Cr FeFe hydrogenase using the method previously established.[35] The mutant is stable and has 30% of the H_2 production activity of the WT. It can be grafted on an electrode just like the WT, and in the absence of O_2 it gives electrochemical signals that are very similar to the WT (compare Figures 4A–C and 6A–C). The mutant *irreversibly* inactivates under anaerobic conditions about twice as fast as the WT (the values of $k_{irrev}^{@0V}$ determined by fitting the CVs were the following: Cr WT, 3 ± 1 × 10^{-4} s^{-1}; Cr T226K, 7 ± 1 × 10^{-4} s^{-1}; Ca WT, 3 ± 2 × 10^{-6} s^{-1}), but we observed no significant difference in terms of kinetics of reversible, anaerobic inactivation. Figure 6D shows the analysis of the aerobic inhibition experiments with T226K, from which we determined the values in Table 1 (third row). The mutation has no significant effect on k_i, and it slightly decreases the rate of O_2 unbinding (k_a). The only beneficial effect is that it makes the reaction slightly more reversible (by decreasing k_3, but only less than 2-fold), and this happens to compensate for the decrease in k_a, so that the mutation has no effect on the apparent bimolecular rate constant of irreversible inactivation $k_i k_3/(k_3 + k_a)$.

3. DISCUSSION

We have developed and used a novel method for precisely characterizing the complex kinetics of oxidative inhibition of FeFe hydrogenases. It consists in using direct electrochemistry to monitor the change in H_2 oxidation current against time, when the enzyme is repeatedly exposed to "bursts" of O_2. The full kinetic model that we used is summarized in eq 2. It considers the reversible and bimolecular formation of an O_2 adduct (rate k_i), which evolves by either giving back the active form (k_a) or by being irreversibly transformed into a dead-end state (rate k_3). Fitting this model to data such as those in Figure 2 would not be difficult if an anaerobic inactivation did not make the current decrease in a complex manner even before O_2 is added. That this inactivation is particularly fast in the case of Cr hydrogenase had prevented us from studying the aerobic inactivation of this enzyme.

We now know that anaerobic inactivation of FeFe hydrogenase is a complex process resulting from the reversible and irreversible formation of several inactive states which are protected from O_2 as depicted in Figure 7. The species labeled 1H and 2H are reversibly formed from Hox upon oxidation in the presence of hydrogen, following an isomerization step that changes the coordination sphere around the distal Fe.[29] The reversible formation of 1H and 2H competes with the oxidative formation of an unknown state called Hoverox, which results in the destruction of the cluster.[29] Anaerobic inactivation cannot be avoided if one is interested in aerobic inhibition, because the electrode potential must be set to a value that is positive with respect to SHE in order to avoid direct O_2 reduction on the graphite electrode that supports the enzyme. There is no difficulty in writing the model that considers all inactivation processes simultaneously, the problem is to make sure that all kinetic parameters are well determined, when they are simultaneously adjusted in the fitting procedure. We solved this indetermination problem by running experiments in the

DOI: 10.1021/jacs.5b06934
J. Am. Chem. Soc. 2015, 137, 12580–12587

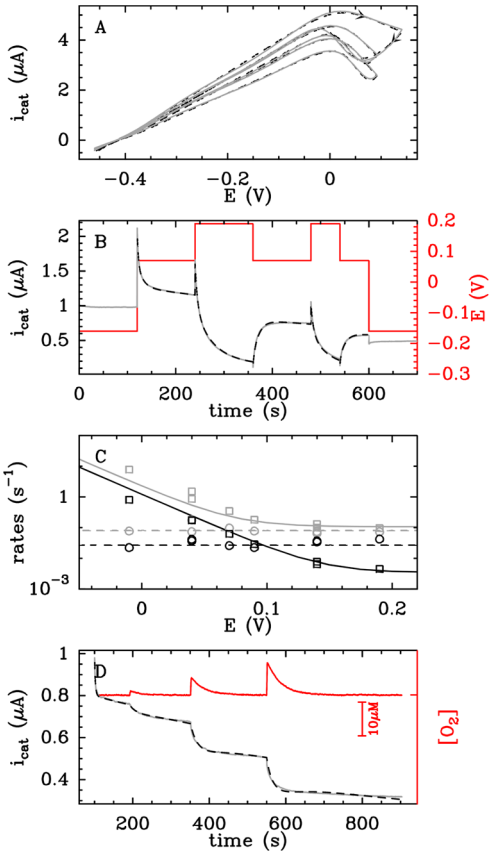

Figure 6. Characterization of the anaerobic/aerobic inactivation of T226K Cr hydrogenase grafted on rotating electrode, T = 12 °C, pH = 7, ω = 3000 rpm, 1 bar H_2. (A) Cyclic voltammograms at different scan rates (20, 5, and 2 mV/s; gray lines) and fits (dashed black lines). (B) Current response of H_2-oxidation (gray line) and fit (black dashed line) for a sequence of potential steps applied to the electrode (red line). (C) Potential dependence of the rate constants for the anaerobic inactivation, extracted from fits shown on panel A ($k'_a(E)$ and $k''_a(E)$, plain lines and $k'_i(E)$ and $k''_i(E)$, dashed lines) and panel B ($k'_a(E)$ and $k''_a(E)$, square dots and $k'_i(E)$ and $k''_i(E)$, circle dots). The rate constants for two species involved in the kinetic model are distinguished using black and gray plots. (D) Catalytic current of H_2-oxidation changes with enzyme exposure to O_2 (gray line), E = 40 mV; $[O_2]_0$ = 1.25 μM, τ = 26 s; 5.1 μM, 33 s; 9.6 μM, 35 s. The oxygen reduction current is plot against time as a red line, E = −560 mV; ω = 6000 rpm.

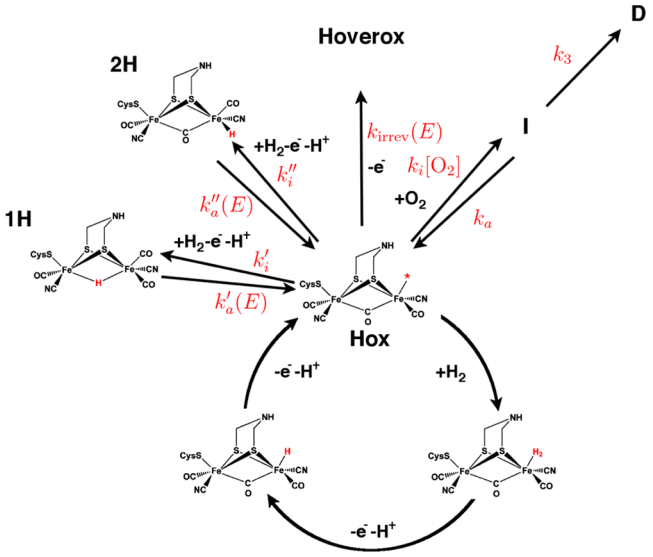

Figure 7. Inactivation of the H-cluster of hydrogenase under oxidizing aerobic and anaerobic conditions. k'_i and k''_i are the first-order, potential-independent rate constants for the reversible formation of 1H and 2H from Hox. The corresponding rates of reactivation k'_a and k''_a depend on potential as shown in, for example, Figure 4C. The rate of formation of the irreversibly inactivated state "Hoverox", $k_{irrev}(E)$, is potential-dependent; it equates $k_{irrev}^{@0V}\exp(FE/2RT)$ (cf. section S1.2 and Figure S4 of ref 29) . The rate constants relative to the aerobic transformation of Hox are discussed in the text. Note that other inactivation reactions, not depicted here, occur under reductive conditions.[38]

absence of O_2 to independently determine all the parameters that describe anaerobic inhibition (e.g., Figure 4A–C), and by using a new setup where a second rotating disc working electrode reports on the instant concentration of O_2 in the electrochemical cell (Figure 2A). By constraining the fitting procedure in this manner, the aerobic data could be analyzed by adjusting a very small number of parameters, which are now well-defined.

From the kinetic traces obtained upon briefly exposing Ca FeFe hydrogenase to O_2 (black line in Figure 2, and Figure 5D), it is very clear that the inhibition is partly reversible. This reversibility had been observed in our previous studies of the FeFe hydrogenases from Ca and *Desulfovibrio desulfuricans* (Dd),[11,12] but it has been disregarded in all subsequent studies of the aerobic inhibition of FeFe hydrogenases. The partial reversibility cannot be detected in experiments where the concentration of O_2 is constant (since in that case, the irreversible destruction (k_3) of the reversibly inactivated enzyme results in an overall irreversible inactivation with an apparent rate constant that equates $k_ik_3/(k_3 + k_a)$), and indeed, based on such experiments, Armstrong and co-workers concluded that the reaction of Dd, Cr and Ca FeFe hydrogenases with O_2 "is essentially irreversible".[36] Looking at the gray kinetic trace in Figure 2, obtained with Cr hydrogenase, it does indeed seem that the inhibition is irreversible, but the best fit of the model that assumes irreversible reaction with O_2 is very bad (dotted line in Figure 4D). This demonstrates that the reversibility of the inhibition has to be taken into account with both enzymes, and, importantly, that the same two-step mechanism applies in both cases: reversible formation of an O_2 adduct (with second-order rate constant k_i and first-order rate constant k_a) and irreversible follow up reaction (first-order rate constant k_3). The difference between the O_2 sensitivity of the two enzymes is therefore quantitative rather than qualitative.

All previous computational studies of the inhibition of hydrogenases have aimed at explaining the alleged irreversibility of the reaction, by hunting for dead-end products. It will be interesting in the future to use theoretical calculations to better understand this reversibility issue, which may be a key to engineer O_2-resistance in this family of enzymes.

Defining the kinetics of the reaction with O_2 should help elucidate the reason O_2-sensitivity varies so much between homologous FeFe-hydrogenases.[11,12,36] Table 1 compiles the values of k_i, k_a, and k_3 obtained in our earlier work and this work, together with the values of the apparent bimolecular rates of aerobic inhibition measured by others, in experiments where the different steps of the reaction with O_2 cannot be distinguished. Although the methods (electrochemistry versus FTIR spectroscopy), experimental conditions (pH, T, E), exact

DOI: 10.1021/jacs.5b06934
J. Am. Chem. Soc. 2015, 137, 12580–12587

values of the rate constants, and level of detail that is achieved vary, there is a consensus about O_2 sensitivity decreasing in the order Dd ≈ Cr ≫ Ca. That there exists significant differences is surprising since the H-cluster and its environment are very conserved. The analysis herein is an important progression of earlier approaches because the three rate constants that define the reaction with O_2 are now measured for the first time with two distinct hydrogenases, using a very rigorous method.

From the fit of model to the aerobic data obtained with Cr and Ca hydrogenases, we conclude that the binding of O_2 is only twice faster for Cr hydrogenase than for Ca hydrogenase and the rate of reactivation (k_a) is the same. The difference between the two enzymes is therefore not related to the initial O_2 binding/release step. Instead, the much greater O_2 sensitivity of Cr hydrogenase (cf. Figure 2) mainly comes from k_3 (the rate of formation of the dead end from the O_2 adduct) being 10 times greater than that for the enzyme from Ca, which makes the reaction with O_2 of Cr hydrogenase much less reversible than that of Ca hydrogenase.

By being able to measure the kinetic parameters that quantify the reaction with O_2 we can now also examine the effect of mutations. In a theoretical study of O_2 binding to the distal Fe of the H-cluster, Blumberger and co-workers suggested that the mutation of residues in the neighborhood of the cubane cluster into positively charged amino acids such as lysine (Figure 1) should stabilize the negative charge on the cubane and make O_2 binding less favorable. In a first attempt to use proteic engineering to increase the O_2 resistance of Cr FeFe hydrogenase, we purified and characterized a mutant where a nonconserved threonine whose side-chain points toward the cubane is replaced with a lysine. This T226K mutant is active (its turnover rate in the direction of H_2 production is 30% of that of the WT), showing that the mutation has little impact on the catalytic properties of the H-cluster, but the effect on the reaction with O_2 is small and not in the direction that was expected. The mutation does alter k_a and k_3, but the effects compensate each other, and the mutation has no effect on the apparent bimolecular rate constant of irreversible inactivation $k_i k_3/(k_3 + k_a)$. This shows that either the mutation does not affect the rate of fixation of O_2, unlike speculated based on the calculations carried out with the wild type enzyme, or that the rate of O_2 binding is determined by factors such as intramolecular diffusion which are independent of the redox state of the H-cluster, and which were not taken into account in calculations. Other authors have calculated that replacing the conserved Thr137 or Ser193 (Cr numbering) with alanine should weaken O_2 binding; we shall test these hypotheses.

The fact that mutations do not have the impact that could have been expected based on theoretical calculations shows that a better understanding of the molecular mechanism of the inhibition by O_2 and the knowledge of which step limit the rate of this reaction are still needed before we can look for mutations that will really increase O_2 resistance. In any case, the comparison between Ca and Cr hydrogenases here shows that differences in amino acid sequences can make O_2 sensitivity vary greatly, and demonstrate the large potential for improvement of the enzyme from Cr. Increasing the resistance of this enzyme is an important goal, considering that Cr is an algae that has great potential in the context of biological, photosynthetic H_2 photoproduction.[8]

The experiments presented here cannot discriminate between the hypotheses of Haumann et al. and Peters et al., because we have examined the early stages of the reaction with O_2 whereas they looked at the final product(s). At this point, we can only speculate about the nature of the dead-end species "D" that is produced upon reaction with O_2, and the reasons the hydrogenases from Ca and Cr react at different rates, despite the fact that the environment of the H-cluster is so conserved. It cannot be excluded that the auxiliary clusters present in Ca play a role in making the enzyme more resistant than Cr; our results show that this would be by preventing the irreversible reaction (k_3), not by favoring O_2 release. We are currently examining in details the effect of all experimental parameters on the values of the three rate constants that describe the reaction with O_2, and the effect of other point-mutations around the H-cluster, in an attempt to learn about the molecular mechanism of inhibition. We hope that, thanks to the methods exposed in this paper, subsequent studies will finally elucidate the mechanism of this important reaction, which is still a hot topic of debate.

4. METHODS

The methods for attaching the enzymes to graphite electrodes,[32] for the aerobic[11] and anaerobic[29] electrochemical experiments, for the purification of the two enzymes[29] have all been fully described previously. A modification of our previous electrochemical setup is the use of a second rotating disc electrode (Figure 3), connected to an Ecochemie PGSTAT12 bipotentiostat. We used gastight Hamilton or SGE syringes to deliver O_2; the error on the concentration depends on the error on the concentration of stock solution, the error in the injected volume and the error in the volume of the buffer in the electrochemical cell, which slowly evaporates. So we assume that the accuracy is around ±5%. We always examined the value of the O_2 reduction current just after the injection to make sure that there was no large (>10%) error. All potentials are quotted with respect to SHE.

The electrochemical data were analyzed using the new homemade, open source program QSoas, which can be downloaded from our Web site (www.qsoas.org), and installed on Windows, Mac OSX, and Linux computers.[39]

We used the approach described in refs 28 and 29 to compute the voltammograms. The current can be written as

$$i(E, t) = i_A(E) \times A(t) \tag{3}$$

where $i_A(E)$ is the steady-state, potential-dependent current response of the active species, and $A(t)$ is the time-dependent fraction of active species.

The potential dependence of the current of the active form was either computed from eq 22 in ref 40 or, when fitting only data at high potentials, using a simple affine dependence on potential.

$A(t)$ is the solution of the following set of differential equations:

$$\frac{dA(t)}{dt} = -[k_i' + k_i'' + k_{irrev}(E(t))]A(t) + k_a'(E(t))I_1(t) + k_a''(E(t))I_2(t) \tag{4}$$

$$\frac{dI_1(t)}{dt} = k_i' A(t) - k_a'(E(t))I_1(t) \tag{5}$$

$$\frac{dI_2(t)}{dt} = k_i'' A(t) - k_a''(E(t))I_2(t) \tag{6}$$

where $I_1(t)$ and $I_2(t)$ are the concentrations of species 1H and 2H, and the rate constants are defined in Figure 7. The potential dependence of $k_{irrev}(E)$, $k_a'(E)$, and $k_a''(E)$ is as follows:[29]

$$k_{irrev}(E) = k_{irrev}^{@0V} \exp(FE/2RT) \tag{7}$$

$$k_a'(E) = k_a'^{@0V} \exp(-FE/RT) + k_a'^{direct} \tag{8}$$

$$k_a''(E) = k_a''^{@0V} \exp(-FE/RT) + k_a''^{direct} \tag{9}$$

DOI: 10.1021/jacs.5b06934
J. Am. Chem. Soc. 2015, 137, 12580−12587

There is no analytical solution for $A(t)$, but its numerical value can be computed using standard ODE integration techniques.

Regarging the production of the T226K hydrogenase mutant of Cr FeFe hydrogenase, site-directed mutagenesis was performed on the CrhydA1 gene cloned into the pBBR-hydA1N vector[35] using Quick Change Site-Directed Mutagenesis Kit (Agilent Technologies, Santa Clara, CA) . The mutagenesis primers used for creating T226K mutant were T226K up 5′-gtccatcatgccctgc**aag**cgcaagcagtc-3′ and T226K down 5′-gactgcttgcg**ctt**gcagggcatgatggac-3′ (with nucleotide triplets coding a mutated amino acid shown in bold). The recombinant plasmid was introduced and expressed in *Shewanella oneidensis* AS52 strain as described in ref 35. An average amount of 0.4 mg of purified active protein per liter of culture was obtained for both native and mutant enzymes. Enzyme purification and activity assay were both performed in a glovebox (Jacomex) filled with N_2. Hydrogen evolution was assayed as described in ref 29.

AUTHOR INFORMATION

Corresponding Author

*christophe.leger@imm.cnrs.fr

Notes

The authors declare no competing financial interest.

ACKNOWLEDGMENTS

The work was funded by the CNRS, Aix Marseille Université, INSA, CEA, Agence Nationale de la Recherche (ANR-12-BS08-0014, ANR-14-CE05-0010), the A*Midex foundation of Aix- Marseille University (project MicrobioE, Grant Number ANR-11-IDEX- 0001-02), Région Provence Alpes Côte d'Azur (PACA), and supported by the "Pôle de compétitivité Capénergie". The authors are part of FrenchBIC (www.frenchbic.cnrs.fr).

REFERENCES

(1) Abbreviations used in this paper: CA: *chronoamperometry*; CV: *cyclic voltammetry*; Ca, *Clostridium acetobutylicum*; Cp, *Clostridium pasteurianum*; Cr, *Chlamydomonas reinhardtii*; Dd, *Desulfovibrio desulfuricans.*

(2) Lubitz, W.; Ogata, H.; Rüdiger, O.; Reijerse, E. *Chem. Rev.* **2014**, *114*, 4081−4148.

(3) Peters, J. W. *Curr. Opin. Struct. Biol.* **1999**, *9*, 670−676.

(4) Silakov, A.; Wenk, B.; Reijerse, E.; Lubitz, W. *Phys. Chem. Chem. Phys.* **2009**, *11*, 6592−6599.

(5) Caserta, G.; Roy, S.; Atta, M.; Artero, V.; Fontecave, M. *Curr. Opin. Chem. Biol.* **2015**, *25*, 36−47.

(6) Hambourger, M.; Gervaldo, M.; Svedruzic, D.; King, P. W.; Gust, D.; Ghirardi, M.; Moore, A. L.; Moore, T. A. *J. Am. Chem. Soc.* **2008**, *130*, 2015−2022.

(7) Wakerley, D. W.; Reisner, E. *Energy Environ. Sci.* **2015**, *8*, 2283−2295.

(8) Ghirardi, M. *Photosynth. Res.* **2015**, *125*, 383−393.

(9) There are exceptions. The enzyme from *Desulfovibrio desulfuricans* can be purified in an inactive form that irreversibly becomes active and O_2 sensitive after reduction.[10] The reason for this has never been fully elucidated.

(10) van Dijk, C.; van Berkel-Arts, A.; Veeger, C. *FEBS Lett.* **1983**, *156*, 340−344.

(11) Liebgott, P.-P.; Leroux, F.; Burlat, B.; Dementin, S.; Baffert, C.; Lautier, T.; Fourmond, V.; Ceccaldi, P.; Cavazza, C.; Meynial-Salles, I.; Soucaille, P.; Fontecilla-Camps, J. C. C.; Guigliarelli, B.; Bertrand, P.; Rousset, M.; Léger, C. *Nat. Chem. Biol.* **2010**, *6*, 63−70.

(12) Baffert, C.; Demuez, M.; Cournac, L.; Burlat, B.; Guigliarelli, B.; Bertrand, P.; Girbal, L.; Léger, C. *Angew. Chem., Int. Ed.* **2008**, *47*, 2052−2054.

(13) Lemon, B. J.; Peters, J. W. *Biochemistry* **1999**, *38*, 12969−12973.

(14) Stripp, S. T.; Goldet, G.; Brandmayr, C.; Sanganas, O.; Vincent, K. A.; Haumann, M.; Armstrong, F. A.; Happe, T. *Proc. Natl. Acad. Sci. U. S. A.* **2009**, *106*, 17331−17336.

(15) Hong, G.; Pachter, R. *ACS Chem. Biol.* **2012**, *7*, 1268−1275.

(16) Yu, L.; Greco, C.; Bruschi, M.; Ryde, U.; De Gioia, L.; Reiher, M. *Inorg. Chem.* **2011**, *50*, 3888−3900.

(17) Stiebritz, M. T.; Reiher, M. *Chem. Sci.* **2012**, *3*, 1739−1751.

(18) Finkelmann, A. R.; Stiebritz, M. T.; Reiher, M. *Inorg. Chem.* **2014**, *53*, 11890−11902.

(19) Kubas, A.; De Sancho, D.; Best, R. B.; Blumberger, J. *Angew. Chem., Int. Ed.* **2014**, *53*, 4081−4084.

(20) Dogaru, D.; Motiu, S.; Gogonea, V. *Int. J. Quantum Chem.* **2009**, *109*, 876−889.

(21) Mulder, D. W.; Boyd, E. S.; Sarma, R.; Lange, R. K.; Endrizzi, J. A.; Broderick, J. B.; Peters, J. W. *Nature* **2010**, *465*, 248−251.

(22) Pandey, A. S.; Harris, T. V.; Giles, L. J.; Peters, J. W.; Szilagyi, R. K. *J. Am. Chem. Soc.* **2008**, *130*, 4533−4540.

(23) Silakov, A.; Kamp, C.; Reijerse, E.; Happe, T.; Lubitz, W. *Biochemistry* **2009**, *48*, 7780−7786.

(24) Lambertz, C.; Leidel, N.; Havelius, K. G.; Noth, J.; Chernev, P.; Winkler, M.; Happe, T.; Haumann, M. *J. Biol. Chem.* **2011**, *286*, 40614−40623.

(25) Swanson, K. D.; Ratzloff, M. W.; Mulder, D. W.; Artz, J. H.; Ghose, S.; Hoffman, A.; White, S.; Zadvornyy, O. A.; Broderick, J. B.; Bothner, B.; King, P. W.; Peters, J. W. *J. Am. Chem. Soc.* **2015**, *137*, 1809−1816.

(26) Léger, C.; Dementin, S.; Bertrand, P.; Rousset, M.; Guigliarelli, B. *J. Am. Chem. Soc.* **2004**, *126*, 12162−12172.

(27) Hamdan, A. A.; Liebgott, P.-P.; Fourmond, V.; Gutiérrez-Sanz, O.; De Lacey, A. L.; Infossi, P.; Rousset, M.; Dementin, S.; Léger, C. *Proc. Natl. Acad. Sci. U. S. A.* **2012**, *109*, 19916−19921.

(28) Fourmond, V.; Infossi, P.; Giudici-Orticoni, M.-T.; Bertrand, P.; Léger, C. *J. Am. Chem. Soc.* **2010**, *132*, 4848−4857.

(29) Fourmond, V.; Greco, C.; Sybirna, K.; Baffert, C.; Wang, P.-H. H.; Ezanno, P.; Montefiori, M.; Bruschi, M.; Meynial-Salles, I.; Soucaille, P.; Blumberger, J.; Bottin, H.; De Gioia, L.; Léger, C. *Nat. Chem.* **2014**, *6*, 336−342.

(30) Greco, C.; Fourmond, V.; Baffert, C.; Wang, P.-h.; Dementin, S.; Bertrand, P.; Bruschi, M.; Blumberger, J.; de Gioia, L.; Leger, C. *Energy Environ. Sci.* **2014**, *7*, 3543−3573.

(31) Adamska-Venkatesh, A.; Krawietz, D.; Siebel, J.; Weber, K.; Happe, T.; Reijerse, E.; Lubitz, W. *J. Am. Chem. Soc.* **2014**, *136*, 11339−11346.

(32) Baffert, C.; Sybirna, K.; Ezanno, P.; Lautier, T.; Hajj, V.; Meynial-Salles, I.; Soucaille, P.; Bottin, H.; Léger, C. *Anal. Chem.* **2012**, *84*, 7999−8005.

(33) Bard, A. J.; Faulkner, L. R. *Electrochemical methods. Fundamental and applications*, third ed.; John Wiley & Sons, Inc.: New York, 2004.

(34) The electroactive coverage of enzyme need not be the same: the current is proportional to the electroactive coverage, but the measurement of the rate constants is based on the relative change in current, and therefore independent of electroactive coverage.

(35) Sybirna, K.; Antoine, T.; Lindberg, P.; Fourmond, V.; Rousset, M.; Méjean, V.; Bottin, H. *BMC Biotechnol.* **2008**, *8*, 73.

(36) Goldet, G.; Brandmayr, C.; Stripp, S. T.; Happe, T.; Cavazza, C.; Fontecilla-Camps, J. C.; Armstrong, F. A. *J. Am. Chem. Soc.* **2009**, *131*, 14979−14989.

(37) Fourmond, V.; Lautier, T.; Baffert, C.; Leroux, F.; Liebgott, P.-P.; Dementin, S.; Rousset, M.; Arnoux, P.; Pignol, D.; Meynial-Salles, I.; Soucaille, P.; Bertrand, P.; Léger, C. *Anal. Chem.* **2009**, *81*, 2962−2968.

(38) Hajj, V.; Baffert, C.; Sybirna, K.; Meynial-Salles, I.; Soucaille, P.; Bottin, H.; Fourmond, V.; Leger, C. *Energy Environ. Sci.* **2014**, *7*, 715−719.

(39) Fourmond, V.; Hoke, K.; Heering, H. A.; Baffert, C.; Leroux, F.; Bertrand, P.; Léger, C. *Bioelectrochemistry* **2009**, *76*, 141−147.

(40) Fourmond, V.; Baffert, C.; Sybirna, K.; Lautier, T.; Abou Hamdan, A.; Dementin, S.; Soucaille, P.; Meynial-Salles, I.; Bottin, H.; Léger, C. *J. Am. Chem. Soc.* **2013**, *135*, 3926−3938.

DOI: 10.1021/jacs.5b06934
J. Am. Chem. Soc. 2015, 137, 12580−12587